Environmental Noise Harvester Using a Helmholtz Resonator and Piezoelectric Transducer

Daniel Aguilar-Torres, Omar Jiménez-Ramírez and Onésimo Flores-Acoltzi

Instituto Politécnico Nacional, Escuela Superior de Ingeniería Mecánica y Eléctrica Unidad Culhuacan, Av. Santa Ana 1000, CDMX, 04430 Mexico.

Juan Antonio Jimenez-Garcia

Universidad Autónoma del Estado de México, Centro Universitario Nezahualcóyotl, Av. Bordo de Xochiaca, Nezahualcóyotl, Estado de México, 57000 Mexico.

Guillermo Luque-Zuñiga and Rubén Vázquez-Medina

Instituto Politécnico Nacional, Centro de Investigación en Ciencia Aplicada y Tecnología Avanzada Unidad Querétaro, Cerro Blanco 141, Querétaro, 76090 Mexico. E-mail: ruvazquez@ipn.mx

(Received 11 April 2022; accepted 28 July 2022)

This work represents a guideline for designing, analyzing, and implementing a compact, low-cost, lightweight, and portable system that harvests energy from environmental noise at different locations. Considering that the proposed energy harvesting system (EHS) is based on a piezoelectric transducer (PZT) embedded in a Helmholtz resonator (HR), we first characterize the noise at four different locations selecting the most suitable ones for energy harvesting. Then, we electrically analyze and describe the PZT determining its resonance frequency. Subsequently, by using this frequency, we perform the sizing of the HR. Thus, we analyze the behavior of the implemented EHS under controlled and actual conditions. In controlled conditions, we determine the gain of the implemented EHS using a pure sinusoidal signal at 500 Hz and a pink noise signal. In actual conditions, we measured its gain considering two different locations. We observed that under controlled conditions, the implemented EHS achieved a gain between 168.3% and 200.3%, and under actual conditions, its gain was 159.5% in the traffic zone and 597.7% in the music zone. In addition, for the HR modeling and design, we show that its theoretical gain corresponds to its simulation gain but differs from its experimental gain due to the used material and manufacturing. Finally, we show that the implemented EHS performs similarly or better than other more sophisticated systems or systems with more piezoelectric elements.

NOMENCLATURE

HR	Helmholtz resonator.
EHS	Energy harvesting system.
PZT	Piezoelectric transducer.
PVDF	Polyvinylidene fluoride.
DPZE	Direct piezoelectric effect.
AEH	Acoustic energy harvester.
EHM	Energy harvester module.
ESM	Energy storage module.
S	Selector.
RB	Rectifier bridge.
BB	Battery bank.
dI	Intensity of the noise.
df	Arbitrarily small frequency bandwidth.
ψ	Spectral distribution of noise.
(f_1, f_2)	Frequency bandwidth.
I	Total noise intensity.
τ	Time interval.
SIL	Spectrum intensity level.
I_{ref}	Reference intensity.
IL	Sound intensity level.
IL_{Max}	Maximum sound intensity level.
IL_{Aver}	Average sound intensity level.
IL_{Min}	Minimum sound intensity level.
Z	Impedance.
V_{PZT}	Piezoelectric transducer voltage.
R_{ref}	Reference resistance.
V_{amp}	Amplifier voltage.
A	Transverse area of the neck.
L	Length of the neck.
l	Effective length of the neck.
V	HR Chamber volume.
SP	Sound pressure.
m	Mass.
k	Spring.
f	Resonance frequency.
c	Speed of the sound.
R	Radius of A.
K	Amplification factor of HR.
SP_{cavity}	Cavity sound pressure.
SP_{incident}	Incident sound pressure.
P_{ref}	Reference pressure.
v_0	Output voltage.
v_i	Input voltage.
$v_0[s(t)]$	Output signal voltage.
$v_0[n(t)]$	Output pink noise voltage.
MAM	Mechanical amplification module.
$s(t)$	Pure signal.
$n(t)$	Pink noise signal.

$v_i[s(t)]$	Input signal voltage.
$v_i[n(t)]$	Input pink noise voltage.
γ	Effective gain.
$\gamma_{s(t)}$	Signal effective gain.
$\gamma_{n(t)}$	Pink noise effective gain.
K_m	Measured amplification gain.
$v_i[m(t)]$	Music location voltage.
$v_i[g(t)]$	Vehicular traffic voltage.
$\gamma_{m(t)}$	Music effective gain.
$\gamma_{g(t)}$	Vehicular traffic effective gain.

1. INTRODUCTION

Nowadays, the growing demand for electricity and the destruction of the environment has driven the development of energy harvesting systems, which harvest clean or renewable energy, complying with conditions and regulations that guarantee environmental conservation. Therefore, we consider the development of practical energy harvesting technologies essential, including not only engineering disciplines but also those oriented towards sustainability and the use of clean and renewable energy sources. In these technological developments, we must also assume the use of techniques and methodologies associated with life cycle analysis, pollution prevention, and, in general, the reduction of environmental degradation.

Clean energies can be harvested by using hydroelectric, wind, solar, oceanic, and geological systems. This kind of energy represents approximately 26.5% of the energy generation worldwide, of which 16.4% is produced by hydroelectric systems, 5.6% by wind systems, 1.9% by photovoltaic systems, 0.4% by geothermal and oceanic systems, and the rest by biomass systems.[1]

On the other hand, one of the biggest problems facing the society of large cities worldwide is the pollution by the environmental noise produced by industrial or commercial activities, vehicles, and loud music, among others. The environmental noise can cause a high concentration of energy, which can be harvested, stored, and applied as electric energy. Although the amount of energy harvested from environmental noise is minimal, it can benefit applications with low power demand. This system scavenges from the primary energy source to obtain power levels in the order of nW-mW. Harvesting energy from environmental noise is a tough challenge to address. But piezoelectric transducers can harvest the voltage differentials produced by an external mechanical force. Hence, energy harvesting systems are a promising technology mainly used in battery-less appliances (body sensor networks or inaccessible remote systems). The performance and effectiveness of an environmental harvesting system (EHS) depend on two aspects: i) the quality of a piezoelectric transducer (PZT) associated with the properties of the materials used to build it, and ii) the transduction mechanism associated with the performance of the small-scale mechanical oscillators that are used in the configuration of the PZT.[2]

In this way, we propose in this work a theoretical-practical guideline for the design, analysis, and implementation of an EHS based on a PZT embedded in a Helmholtz resonator (HR) tuned at 500 Hz. Thus, we implement an EHS to generate electricity by harvesting the environmental noise through a mechanical amplifier consisting of a PZT embedded in an HR. To analyze the implemented EHS, we first define a system behavior and functionality baseline using acoustic test signals under controlled conditions. In this sense, we highlight that other authors have used test acoustic signals greater than 100 dB.[3–7] The proposed theoretical-practical guideline consists of the following working stages: i) Requirements analysis, ii) Functional description of the proposed EHS, iii) Design and implementation of the proposed EHS, iv) Experimental setup and testing, and v) Comparison of the proposed EHS against similar systems.

Therefore, this work includes the following sections. Section 2 provides the details of the contribution of this work. Section 3 shows the works related to energy harvesting using PZTs. Section 4 describes the proposed practical guideline to design, analyze, and implement an EHS. Section 5 shows a general description of the proposed system considering the PZT, the HR, and the energy storage module. Section 6 firstly, Subsection 6.1 defines how environmental noise should be treated, assuming its variations in time and frequency. It defines the circuit used to quantify the sound intensity level of the environmental noise at four locations. Subsection 6.2 shows the characterization of the used PZT, and, finally, Subsection 6.3 presents the modeling and design of HR considering the behavior and performance profile of the used PZT. Section 7 describes two experimental scenarios to evaluate the proposed system. In particular, Subsection 7.1 shows the experimental results for the proposed system under controlled conditions, and Subsection 7.2 shows the experimental results under the real condition. Section 8 presents the challenges and discussions about the proposed guideline and the designed and implemented EHS. Finally, Section 9 is devoted to the conclusions for this work.

2. WORK CONTRIBUTION

Whereas other works are focused on energy harvesting from transportation systems (trains and airplanes),[8,9] road tunnels,[10] or acoustic signals produced in controlled processes,[3,6,7] in this work, we are focused on proposing a theoretical-practical guideline to design, analyze, and implement a compact, inexpensive, lightweight, elementary, low-capacity EHS for harvesting energy from environmental noise at four different locations: people talking, schools, music zones, and vehicular traffic locations. The proposed guideline consists of five working stages: i) Design requirements, ii) System functional description, iii) System design and implementation, and iv) Experimental setup and testing. Specifically, in the experimental setup and testing stage, we analyze the behavior of the proposed EHS under controlled and actual conditions. Also, as a preliminary activity, in this working stage, we compare the theoretical, simulation, and experimental gains obtained for the HR used in the proposed EHS. It is emphasized that the implemented EHS has 10 cm $\times$ 10 cm $\times$ 15 cm in size, and when it is calibrated and evaluated in an experimental setup under controlled conditions, it was excited with an acoustic signal at 500 Hz and 90 dB produced from a distance of 1 m from the HR. When the implemented EHS was analyzed under actual conditions, we showed that it allowed quantifying the amount of noise that can be harvested at the considered locations by selecting the two points from which the most energy was harvested. Finally, in contrast to the results reported by other authors, we demonstrate that the implemented EHS is feasible to

be applied since it gathers an amount of energy comparable to that harvested by other systems.[5]

On the other hand, this guideline is also directed to students and professionals involved in designing and implementing electronic systems to enhance their understanding of EHSs that harvest energy from ambient noise. As seen from Section 4, the proposed guideline offers a simple and practical approach to analyzing, designing, and implementing an EHS that harvests energy from environmental noise. The procedure followed in this guideline is intended to maintain the technological perspective by identifying the need and requirements to be considered when solving a specific problem involving using an EHS that harvests energy from environmental noise.

3. RELATED WORKS

An environmental harvesting system typically uses the energy produced by the wind, tides, earthquakes, and the human body, among others to produce electricity.[11–15] However, other energy harvesting options can be technologically and financially feasible in applications of low energy consumption. Several works have been reported considering environmental noise as a regenerative energy resource that can be harvested to generate electricity. For example, a noise barrier was developed to harvest renewable acoustic energy using an HR and a polyvinylidene fluoride (PVDF) film to convert the acoustic energy of low-frequency noise from high-speed rail tracks into electricity.[8] It should be considered that the energy harvesters based on piezoelectric vibration produce high energy density for practical applications.[16] From the piezoelectric effect discovered by the Curie brothers in 1880,[17] using PZTs to harvest clean and sustainable energy has had extensive technological development. PZTs have become a viable option for energy harvesting from mechanical vibrations by exploiting the direct piezoelectric effect (DPZE), using materials such as crystals, ceramics, and Rochelle salts.[18] DPZE is generated when one of the faces of the piezoelectric materials is deformed by some mechanical force. Then a dipole is caused by the loss of symmetry in the material generating a potential differential. This phenomenon can also be generated inverse; if an electric field is applied to some of the faces of the piezoelectric material, then a mechanical distortion will cause an electric output. Due to this feature, the PZTs have a dual function. They can be speakers or microphones.[19]

Next, we present a review of works that have contributed to designing energy harvesting devices and systems. Some of these works showed a feasibility study about piezoelectric energy harvesters placed on floors inside buildings.[20] Similarly, a prototype EHS from raindrop was developed in 2017 by Ilyas and Swingler for energy harvesting.[21] Ilyas and Swingler presented the following findings in their work: i) a technique to identify the efficiency of the impact mechanism as the droplet interacts with the device, ii) the efficiency of the mechanic-electric conversion mechanism depends on internal losses in the device, iii) verifying the values for the efficiency of the impact mechanism and the conversion mechanism, and iv) the optimum arrangement for a single device.

On the other hand, Wang *et al.* designed an energy harvester that includes a piezoelectric film placed inside a mechanical resonator for energy harvesting from train noise.[8] In that case, the harvested energy was stored in a supercapacitor. Also, in 2019, Maamer *et al.* presented a reviewing study about the design improvements and techniques for energy harvesters using piezoelectric and electromagnetic schemes.[22] They proposed an improvement approach based on methods to extend the operating frequency of a non-resonant system by using a multidirectional harvester.

In 2019, Sarker *et al.*[23] presented a reviewing study about piezoelectric-based EHSs and optimization techniques to improve their performance. In that work, Sarker *et al.* reviewed two key approaches to designing a piezoelectric-based EHS: mechanical or electronic design. This review focused on numerous challenges and recommendations for next-generation energy harvesters using vibration-based piezoelectric devices. Similarly, a reviewing study about EHSs was presented in 2019 by Choi *et al.*,[24] focusing on fundamental principles, examples, and enhancement methods. Choi *et al.* classified EHSs using two approaches: i) sound pressure amplification based on a resonator and an acoustic metamaterial, and ii) transduction mechanism based on piezoelectric, electromagnetic, and triboelectric mechanisms. Recently in 2021, a review showing the advances in acoustic energy harvesting based on resonant cavities was written by Li *et al.*[5] In this review, they showed the different resonator-PZT configurations used over time and the voltage levels obtained in each of them, ranging from 400 mV to 16 V.

Specifically, about the sound energy harvesters, in 2013, an acoustic energy harvester using a quarter-wavelength straight-tube acoustic resonator with piezoelectric polyvinylidene fluoride (PVDF) beams placed inside the resonator was proposed by Li *et al.*[3] With a single PVDF beam placed inside the tube, they reported that the harvested voltage and power reach a maximum near the open entrance of the tube, where the highest acoustic pressure gradient vibrates the PVDF beam. Li *et al.* also used multiple piezoelectric beams inside the tube with two different configurations: aligned and zigzag. They found that the total output voltage of the piezoelectric beams increases linearly as the incident acoustic pressure increases. Also, in 2013, Li *et al.*[4] developed a low-frequency energy harvesting system consisting of an eight-plate PZT array and a straight tube resonator. Their results showed that the designed system harvested 15.68 V; in that case, they used an acoustic signal of 199 Hz with a sound intensity level of 110 dB under controlled conditions.

On the other hand, in 2015, an EHS from vibrations induced by a jet-resonator system was proposed by Zou *et al.*[16] They developed a piezoelectric-based EHS for powering the electronic aircraft system, which converts the incoming airflow energy into electricity via a PZT during the flight. In 2016, an acoustic energy harvester using tapered neck HR and piezoelectric cantilever undergoing concurrent bending and twisting was presented by Pillai and Ezhilarasi.[6] They demonstrated that an integrated structural modification of the acoustic resonator and PZT in an acoustic energy harvester could augment the overall harvesting efficiency.

In 2017, a work that showed the characterization of PZTs to harvest energy from sound waves was presented by Fang *et al.*[25] They showed that the sound level on PZT was 35–100 dB, comparable with human audible environmental sound (50–100 dB). The output of PZT was connected to three different circuits. i) Villard voltage multiplier, ii) Dickson voltage multiplier, and iii) full-wave rectifier. They showed that the

PZT connected to Villard voltage multiplier produced the best performance for that case. Also, in 2017, Fang *et al.*[26] characterized different PZTs to be used in an energy harvesting system to capture the energy of environmental vibrations; the vibrations obtained were converted into electrical energy and later used in low-power devices. Subsequently, in 2018, Mir *et al.*[27] proposed a metamaterial wall (Meta-Wall) for industrial sound insulation walls. They claimed that the proposed Meta-Wall achieved three main objectives: (1) to provide improved sound insulation capability superior to state-of-the-art technologies, (2) to maintain the structural strength required by design, and (3) to potentially utilize the isolated noise by transforming acoustic energy into usable electrical energy, simultaneously.

Later, in 2018, Wang *et al.*[8] proposed an energy harvester that includes a piezoelectric film placed inside a mechanical resonator for energy harvesting from train noise. Also, in 2018, Noh *et al.*[28] designed an energy harvesting system using noise between 50–200 Hz generated by a high-speed train during practical operation. They obtained an energy harvesting of approximately 0.7 V generated for a sound pressure level of 100 dB using a large rectangular plate embedded in a Helmholtz resonator. In 2019, Ahmad *et al.*[29] developed an acoustic energy harvester (AEH) consisting of two Helmholtz cavities and a commercially available piezo element. They performed various experiments to record the frequency response function, loading, and power characteristics. Their results showed a maximum power density harvested of 32.7 μW/cm^3 at 130 dB. Also, in 2019, Hu *et al.*[30] presented the modeling of membrane-coupled HR and its application in acoustic metamaterial systems. They consider two modes of vibration in the membranes to improve the prediction of the dynamic response of the membrane-coupled HR and the band gap of the acoustic metamaterial system. More recently, in 2020, Eghbali *et al.*[31] proposed an auxetic lattice resonator backed by a rectangular acoustic tube to improve the efficiency of acoustic energy harvesting. They evaluated the energy harvesting performance at different sound power, geometrical aspects, and electrical properties. From the obtained results, they showed that the performance of the acoustic energy harvesting system can be significantly improved at low frequencies (138 Hz) and that in an optimal situation, the system reaches an amplification factor of around 10.5 for an incident sound pressure level of 100 dB.

4. WORK GUIDELINE DESCRIPTION

This work represents a theoretical-practical guideline that aims to design, implement, and analyze an energy harvesting system (EHS) to harvest energy from environmental noise. Following and applying this work guideline, we implemented a functional, simple, compact, efficient, and low-capacity EHS tuned at 500 Hz. The proposed approach has been established as an experimental design framework that guarantees, in the engineered EHS, high utilization of energy resources harvested from environmental noise. Thus, the stages that constitute the proposed theoretical-practical guideline are as follows:

i. **Design requirements.** Two functional requirements must be met to design and implement an EHS. The first requirement is that the HR must be designed from the resonance frequency of the used PZT, ensuring that the HR and the PZT are set at the same operating frequency, aiming to comply with the principle of maximum energy transfer between two devices. The second requirement is related to the EHS's physical dimensions, which depend on its usage and purpose. In this regard, we would like to have a compact, inexpensive, lightweight, elementary, low-capacity EHS, which can be used in a portable way to estimate the energy harvested from environmental noise at different locations where a common person performs daily. Therefore, throughout the different Sections of this work, we show the functional specifications of the HR that must be considered when designing and implementing an EHS to harvest energy from environmental noise. Additionally, using a sound pressure level measurement system, we quantified the environmental noise at considered locations to establish the issues and conditions of the experimental scenarios where energy harvesting from environmental noise can be feasible. Thus, we characterize the environmental noise at each considered location and consider all the variables and parameters necessary for HR to work properly. Considering the generality, for this stage of the proposed guideline, we only consider that the design requirements to be fulfilled for the EHS are to have dimensions of 10 cm $\times$ 10 cm $\times$ 15 cm and to operate at 500 Hz. However, this stage must be done formally considering a strict requirement analysis, the required application, and the specific problem to be addressed. We recommend that the reader reviews the following references[32–34] to clarify this stage of the proposed guideline.

ii. **System functional description**. Section 5 describes the designed and implemented EHS considering its components. Based on this overview, the students and practitioners interested in energy harvesting from environmental noise will be able to understand, analyze, design, and implement each component of an EHS.

iii. **System design and implementation**. In Section 6, we show the theoretical development that must be followed to obtain the necessary parameters when designing an EHS that harvests energy from environmental noise. The basic theoretical concepts fundamentally include the piezoelectric transducer's resonant frequency and frequency response. From this, the Helmholtz resonator is designed and sized so that it couples properly with the transducer allowing us to obtain as much energy as possible from the designed and implemented EHS.

iv. **Experimental setup and testing**. In Section 7, we show the experimental setup that students and practitioners interested in EHS should implement, assuming that each experiment has been designed to measure the energy harvested from environmental noise by using a specific EHS. In this case, we first consider experiments under controlled conditions and later under real conditions. Using this approach, we can have more knowledge and control of the designed and implemented EHS facilitating the quantification and comparison of the harvested energy. In this way, following this approach, students and practitioners will be able to know the functionality of the designed

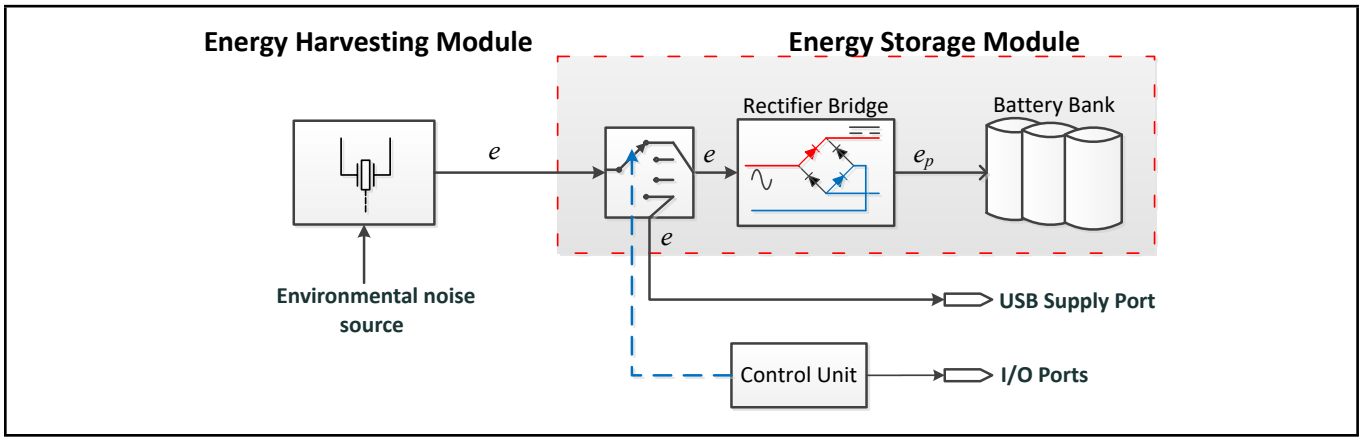

Figure 1. Diagram of the energy harvesting system.

and implemented EHS, and they will have the necessary skills to use it in a real application.

v. **Comparison of the proposed EHS against similar systems**. In Section 8, we show that the proposed EHS is competent in voltage harvesting compared to other systems. We have included Table 4 in order to compare the harvested voltage for the proposed EHS when compared against three implemented EHSs.

From each of the previous stages, students and practitioners interested in EHSs that harvest energy from environmental noise will be able to define experiments and perform the necessary calculations to analyze, design, and evaluate the EHSs that they may develop in the future.

5. SYSTEM FUNCTIONAL DESCRIPTION

EHS implemented in this work consist of two primary modules: i) energy harvesting module (EHM) and ii) energy storage module (ESM), which have been identified in Fig. 1. The implemented EHS has I/O ports linked to the keyboard and display for the control unit, and it has a USB supply port to supply power to any USB device. EHM harvests energy from environmental sound and provides electrical energy to ESM. The implemented EHS includes a selector that sends power to the batteries or the USB supply port as required. The control unit monitors both the ESM port and USB supply port. In the following subsections, the two modules are described in detail.

5.1. Energy Harvesting Module (EHM)

EHM includes an HR that takes advantage of the air resonance phenomenon in a cavity to become an acoustic amplifier. The HR is embedded with a PZT S118-J1SS-1808YB, made of lead zirconate titanate type J5 with a piezoelectric coefficient d_{33} of 500×10^{-12} [C/N], which allows increasing the amplification gain of the EHM reducing the low-frequency noise. Then, when the PZT is embedded in the HR, the effective frequency bandwidth of the EHM may be greater than that achieved when the EHM only includes the HR. In Table 1, we listed the parameters of the PZT S118-J1SS-1808YB.

5.2. Energy Storage Module (ESM)

Firstly, it is worth noting that ESM is the peripheral circuit to the HR. That is, considering that the HR has embedded the PZT, it produces at its output an electrical signal that can be used to power the battery bank (BB) or to provide power to other devices through the USB supply port. Therefore, the ESM is used to store the harvested energy and supply power to electronic devices by using the USB supply port. According to Fig. 1, ESM includes a selector (S), a rectifier bridge (RB), and a battery bank (BB). S allows the power in ESM to be routed considering two possibilities: i) USB supply port and ii) RB and then to BB. RB translates the AC signal e to the DC signal e_p, which will be stored in BB. The ESM is designed to take full advantage of the energy harvested from the EHS. For this purpose, the electronic circuit has a control system that allows, from the selector (S), directing the harvested energy e for use in charging electronic devices through the USB supply port or for energy storing in the battery bank (BB) to be used later in various applications.

Table 1. Parameters of the PZT S118-J1SS-1808YB.

Parameter	Value
Height [mm]	55.4
Width [mm]	23.4
Thickness [mm]	0.46
Output power [mW]	4.4
Temperature range [°C]	–60 to 120
Capacitance [nF]	100
Mass [g]	2.8
Spring constant [N/mm]	0.25
Piezoelectric d_{33} coefficient [C/N]	500×10^{-12}

6. SYSTEM DESIGN AND IMPLEMENTATION

6.1. Environmental Noise

The environmental noise should be treated as an audio signal with time and spectral intensity variations. The spectral distribution of the noise in an arbitrarily small bandwidth can be described according to Eq. 1:

$$\psi = \frac{dI}{df}; \tag{1}$$

where dI is the noise intensity in an arbitrarily small frequency bandwidth df.

Then, the total noise intensity, in a frequency bandwidth (f_1, f_2), is given by Eq. 2:

$$I = \int_{f1}^{f2} \psi \, df. \tag{2}$$

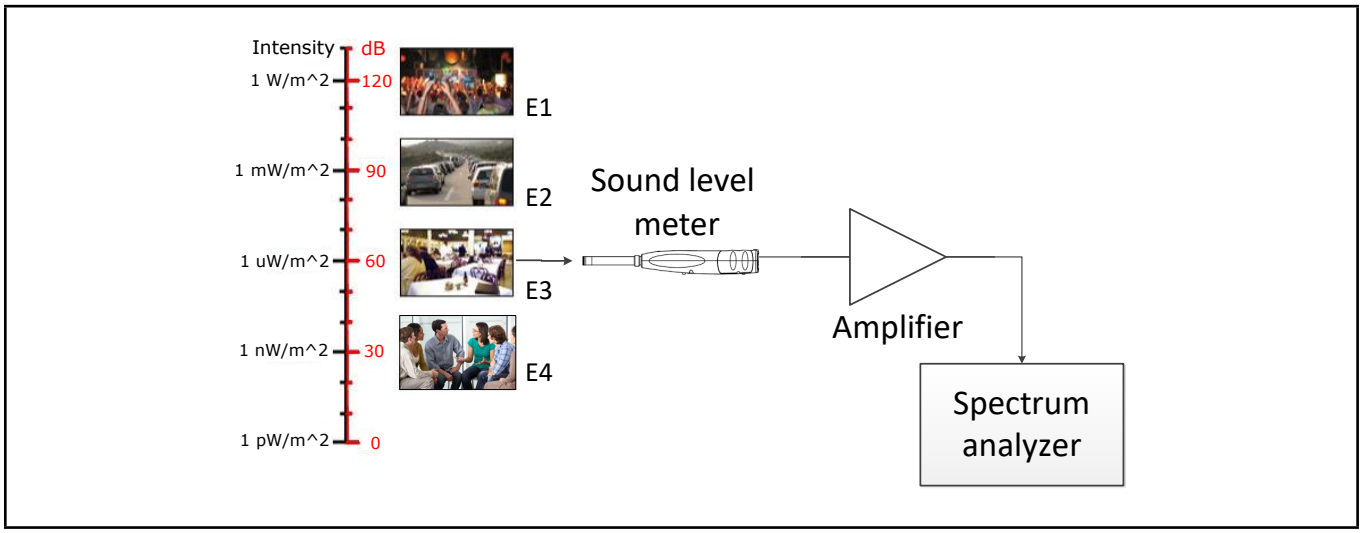

Figure 2. Circuit used to measure environmental noise at four locations: music location (E1), vehicular traffic location (E2), school location (E3), and talking people location (E4).

On the other hand, the time-dependent spectral density varies over time according to Eq. 3:

$$\psi = \langle \psi(f) \rangle_{\tau}. \tag{3}$$

Now, ψ can be expressed in decibels and we calculate the spectrum intensity level according to Eq. 4:

$$SIL = 10 \log \left(\frac{\psi}{I_{\text{ref}}} \cdot 1 \text{ Hz} \right); \tag{4}$$

where $I_{\text{ref}} = 1 \times 10^{-12}$ W/m^2 is the reference intensity in air that approximately corresponds to the threshold of hearing for young persons in the frequency range of greatest sensitivity (1 to 4 kHz).[35]

Although the details about the experiments for obtaining the environmental noise intensity levels were presented by Torres *et al.*,[36] in this case, we use a 1 Hz bandwidth divisor to simplify the notation, since the calculation of the noise intensity is performed in (f_1, f_2) by using Eq. 2.[37] It is important to emphasize that Torres *et al.*[36] showed different noise maps, which served as a reference to establish the procedures and the best locations for noise measurement. Also, they showed the instrumentation circuit for noise measurement, the characteristic noise curves of each analyzed location, the sound intensity levels, and the criteria that they used to select the most suitable place for energy harvesting from environmental noise.[36]

Thus, considering that SIL is frequency dependent, the sound intensity level, IL, can be calculated from Eqs. 1 and 2, according to Eq. 5:

$$IL = 10 \log \left[\frac{I}{I_{\text{ref}}} \right]. \tag{5}$$

Considering Eq. 5, IL can be measured using a calibrated sound level meter and processing the voltage signal obtained from an adjustable filter. Figure 2 shows the electronic circuit used to measure environmental noise.

For energy harvesting from environmental noise, the noise map is essential to quantify the noise levels at available locations.[38] Environmental noise is space-dependent on the noise source, the receiver, and the intervening obstacles (e.g., the terrain, buildings, barriers). So, using the spatial noise variations, it is possible to identify the locations with excessive noise levels. This way, the noise map at available locations identifies where the most energy can be harvested from environmental noise. Table 2 shows the noise levels at different locations[36] indicating the maximum (IL_{Max}), minimum (IL_{Min}), and average (IL_{Aver}) noise levels in dBA from the following locations: vehicular traffic location, school location, music location, and talking people location. The data reported in Table 2 were obtained considering the Mexican Standard NOM-081-ECOL-1994,[39] which establishes that the environmental noise must be measured by using a calibrated sound level meter at different cardinal bearings in a specific day hour. In this way, the data reported in Table 2 were obtained by averaging the sound pressure level considering five measurement events, each of them of 30 seconds, by cardinal bearing by five times.

Table 2. Environmental noise levels.

Location	IL_{Max} [dBA]	IL_{Aver} [dBA]	IL_{Min} [dBA]
Talking people	52.7	39.3	25.6
School	92.7	73.3	70.0
Music	85.5	73.8	42.5
Vehicular traffic	98.0	85.0	74.0

It is emphasized that IL is the amount of energy radiated by a specified source and is measured in dB with respect to I_{ref}. With the results reported in Table 2, IL_{Aver} has been considered to select the locations where the most significant amount of energy is harvested. In this case, we chose the traffic and music locations because their average energy was 85.0 dB and 78.3 dB, respectively, when the energy was harvested using the implemented EHS. Considering its lower and upper limits, we should note that the sound intensity level of environmental noise at the school location shown in Table 2 can be higher than that of the sound intensity level of environmental noise at the other sites. However, this location was not considered because it can be a null source of environmental noise during vacation periods and holidays.

6.2. Piezoelectric Transducers Characterization

Considering that PZTs are electroacoustic devices,[19,40] we can characterize them based on their frequency response and resonance frequency. Thus, beginning with the resonance fre-

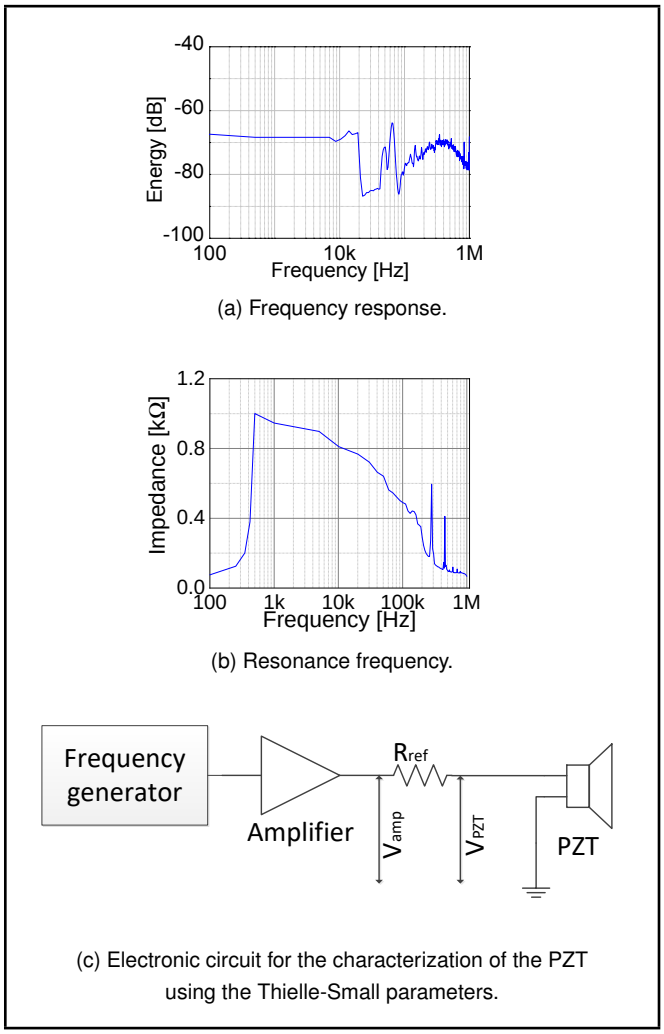

Figure 3. Characterization of the PZT S118-J1SS-1808YB.

quency of the PZT, we can design the HR required in the EHS. Therefore, the methodology needed to measure these features for a PZT is shown below.

Hence, to estimate the frequency response of a PZT, we use a spectrum analyzer connected to a sound level meter calibrated to 1 kHz, 1 W, and 90 dB located 1 m from the PZT. Then, the PZT is excited with a pink noise signal. The frequency response for the PZT S118-J1SS-1808YB used in this work is shown in Fig. 3(a). It is worth noting that the frequency response of this PZT is approximately constant up to 20 kHz, and then it has important variations that would limit its use in that frequency range. Thus, it should be noted that this PZT can be used reliably with frequencies from 1 to 20 kHz.

Figure 3(a) shows the frequency response of the PZT. We should note that the PZT has a good response in the sound bandwidth, but in the ultrasound band, this PZT can take advantage of a wide bandwidth for energy harvesting. Also, in Fig. 3(b), we show the resonance frequency measured using the Thiele-Small circuit[41,42] on the PZT used in this work. The Thiele-Small circuit shown in Fig. 3(c) allows to obtain the impedance variation of the PZT in bandwidth from 1 Hz to 1 MHz using a fine sweep of frequencies with a measuring step of 100 Hz and considering a reference resistance $R_{\text{ref}} = 1$ kΩ. We should note that the resonance frequency of the PZT depends on the voltages measured at the output of the amplifier and the current on the resistance R_{ref}.[43] In the resonance frequency, the impedance obtained is purely resistive, and it occurs when the imaginary part is zero. Therefore, the voltage and current will be in phase, and by Ohm's law, the impedance for the transducer is calculated according to Eq. 6:

$$Z = \frac{V_{\text{PZT}} R_{\text{ref}}}{V_{\text{amp}} - V_{\text{PZT}}}. \tag{6}$$

Considering Eq. 6 and the Thiele and Small circuit, we perform a fine sweep of frequencies with a measuring step of 100 Hz, and we measure the voltages of the amplifier and PZT for each frequency to calculate the R_{ref} and impedance for each frequency.

6.3. Modeling and Design of Helmholtz Resonator

Helmholtz resonators (HRs) are devices that help absorb mechanical waves and are mainly used to reduce the noise at different bandwidths. However, HRs are also considered mechanical amplifiers of acoustic signals.[44,45] An HR consists of a chamber and a neck-shaped inlet attached to it. The HR chamber is a small closed spherical cavity with a hole connecting to the HR neck, which is a small tube with both ends open. The coupling of these two components makes the HR works as a simple oscillator in which the HR chamber acts as a spring, and the HR neck acts as a mass.[46–48] The mass-spring system that describes the HR is shown in Fig. 4. Here, A is the transverse area of the HR neck, L is the length of the HR neck, l is its effective length, r is the radius of the transversal area of the HR neck, R is the radius of the HR chamber, V is the volume of the HR chamber, SP is the sound pressure, m is the mass, and k is the spring constant.

It should be noted that the analogy of a spring-mass system with the HR, shown in Fig. 4, comes from the fact that the air contained in the volume of the HR chamber acts as a spring of constant k, which is attached to the air mass m contained in the HR neck. When a disturbance force SP is applied to the air mass contained in the HR neck, a change in pressure is produced inside the HR chamber, describing a simple harmonic motion, the same motion described by a spring-mass system. The mathematical relationship between the HR and a spring mass system is shown in Eqs. 7 and 8, where Eq. 7 describes the free oscillating spring-mass system without damping, and Eq. 8 describes the dynamics of the HR from the net force SP moving the air mass m inside the HR chamber:

$$m\frac{d^2x}{dt^2} + kx = 0; \tag{7}$$

$$m\frac{d^2x}{dt^2} + SP\frac{A^2}{V}x = 0. \tag{8}$$

The basic resonance frequency of the HR in response to the incident sound pressure crossing the neck is given by Eq. 9:

$$f = \frac{c}{2\pi}\sqrt{\frac{A}{V \cdot l}}; \tag{9}$$

where f is derived from the characterization of the used PZT, and c is the sound speed in air (343 m/s at 20 °C).

For the HR, considering that the implemented EHS should be portable and small in size, we assumed that $r = 0.02$ m and

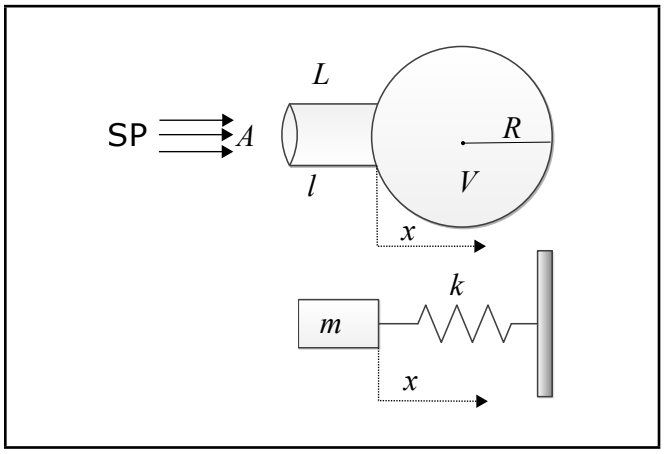

Figure 4. Model of the HR and mass-spring system.

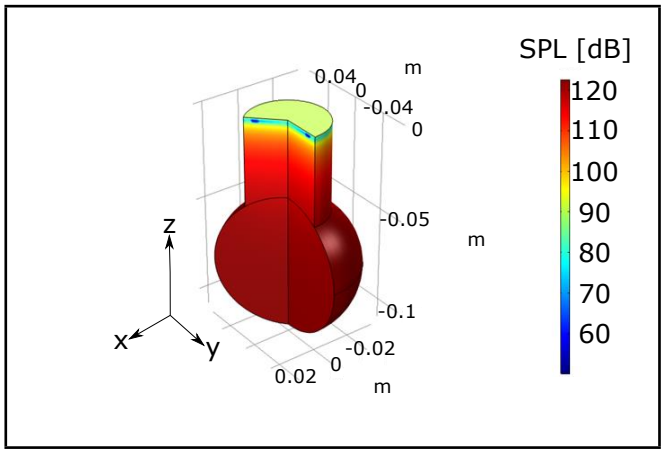

Figure 5. Simulation for the SPL inside the designed HR.

Table 3. Dimensions of the implemented HR when the resonance frequency is $f = 500$ Hz.

Parameter	Dimension
A	1.256×10^{-3} m^2
L	50×10^{-3} m
l	78×10^{-3} m
V	1.922×10^{-4} m^3

$R = 0.05$ m, and then, we calculated the transverse area of the HR neck by using Eq. 10 and the HR chamber volume by using Eq. 11:

$$A = \pi r^2; \tag{10}$$

$$V = \frac{4}{3}\pi R^3. \tag{11}$$

Thus, l can be calculated from Eq. 9 and, consequently, L is calculated from Eq. 12:[46]

$$l = L + 1.4r. \tag{12}$$

In this way, in Table 3, we showed the dimensions of the HR calculated by using Eqs. 9 to 11.

Considering V, l, and A, and assuming that we designed the HR from the resonance frequency, $f = 500$ Hz, of the used PZT (see in Fig. 3(b)), we used Eq. 13. This equation considers the ratio between SP inside the cavity (SP_{cavity}) and SP incident passing through the neck (SP_{incident}) to determine that the HR amplifies by K the sound pressure level of the signal generated by the acoustic source:

$$K = \frac{SP_{\text{cavity}}}{SP_{\text{incident}}} = 2\pi\sqrt{\frac{l^3 \cdot V}{A^3}}. \tag{13}$$

Therefore, using Eq. 13, we estimated the experimental amplification gain, $K_e = 42.63$. On the other hand, we can also estimate the simulation amplification gain, K_s, considering the parameter values reported in Table 3. Thus, assuming that the sound pressure level in chamber center of the HR was $SPL_{\text{cavity}} = 123$ dB, or equivalently $SP_{\text{cavity}} = 28.25$ Pa, and the incident sound pressure level in the HR neck was $SPL_{\text{incident}} = 90$ dB, or equivalently $SP_{\text{incident}} = 632.45$ mPa, the simulation amplification gain is $K_s = 44.66$, which is 1.05 times K_e. It is worth noting that the values of SPL were obtained from the simulation shown in Fig. 5. Additionally, note that SPL is a measure of the root mean square pressure of a sound, and it is calculated by $SPL = 20\log(P/P_{\text{ref}})$, where P_{ref} is a reference pressure. For air, $P_{\text{ref}} = 20$ μPa corresponds approximately to the threshold of hearing for young people in the frequency range of 1 to 4 kHz.

In Fig. 5, we show the simulation of the implemented HR by using COMSOL Multiphysics™, which is a software that uses the finite element method to solve ordinary and partial differential equations. Among its various uses, this software is helpful in mechanical engineering applications for acoustics-related analysis, providing tools for modeling the propagation of mechanical waves in fluids and solids. In this way, we perform the simulation considering the HR dimensions, conditions of the medium through which the wave propagates, and the input signal mentioned above. In Fig. 6, we show the implementation of the HR designed by using SolidWorks™ and manufactured by using a 3-D printer.

7. EXPERIMENTAL SETUP AND TESTING

In Fig. 7, we show a general diagram of the experimental setup for the designed EHS when it is implemented to harvest energy from environmental noise. This diagram includes four components: an acoustic source, a mechanical amplifier, a data acquisition module (DAQ module), a sound level meter, and a personal computer (PC) for data processing. For the DAQ module, we used the DAQ Analog Discovery 2 of Digilent, Inc. We used the sound level meter to measure the sound pressure generated by the acoustic source. In Fig. 7, we show the mechanical amplifier allows two amplification options: i) by using a PZT or ii) by using a PZT embedded into the implemented HR. Note in Fig. 7 two equivalent voltages: the equivalent input voltage (v_i) and the equivalent output voltage (v_o) at the mechanical amplifier module. It is worth noting that v_i and v_o will be used in the Subsection 7.1 to compute the relative gain of the mechanical amplifier module for two cases. On the other hand, in Fig. 8, we show the experimental setup to evaluate and test the designed and implemented EHS considering two energy harvesting scenarios: a) under controlled conditions and b) under real conditions.

We now proceed to explain the energy harvesting from environmental noise for the two scenarios mentioned above.

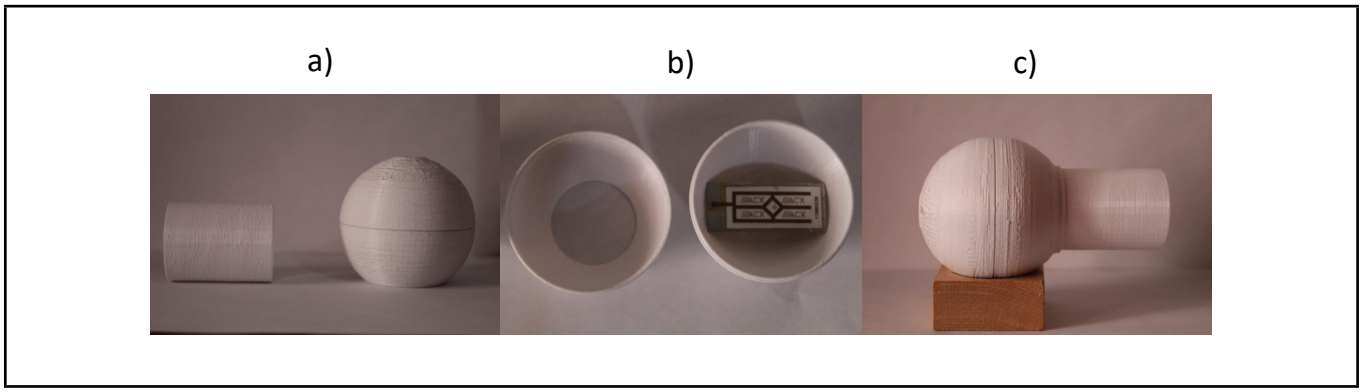

Figure 6. Helmholtz resonator: a) HR neck and chamber, b) PZT embedded inside of the HR, and c) Assembled HR.

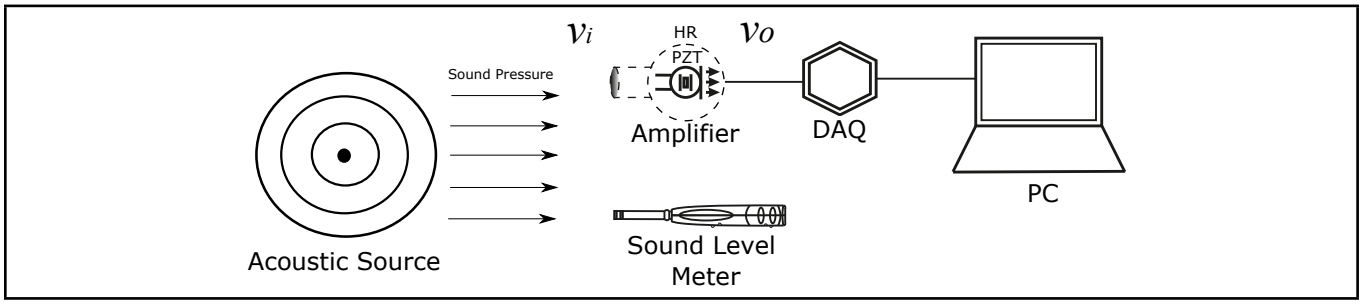

Figure 7. General diagram of the experimental setup proposed to evaluate and test the energy harvested from environmental noise.

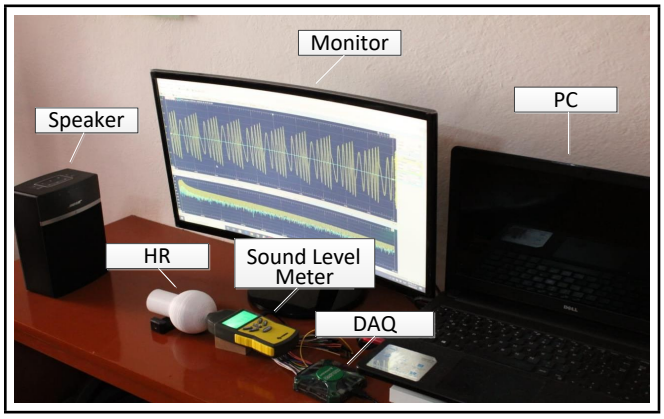

Figure 8. Implementation of the experimental setup proposed to evaluate and test the energy harvested from environmental noise.

7.1. Energy Harvesting under Controlled Conditions

To show the energy harvesting from environmental noise under controlled conditions, we defined two experimental approaches, in which the acoustic source generates acoustic signals with a sound pressure level of 90 dB. In the first approach, we generated a pure sinusoidal signal at 500 Hz, and in the second approach, we generated pink noise signals. The acoustic signals are generated in both methods using a function generator, an electric signal amplifier, and a loudspeaker. Note that we measured the sound pressure level using the sound level meter and acquired the electrical signals from the output of the mechanical amplifier by using the DAQ module. Then we processed the outputs by using a PC.

In Fig. 9, we showed the voltages harvested by the mechanical amplifier module (MAM) considering the two approaches: i) using a PZT (Fig. 9(a)) and ii) using an HR with a PZT embedded in it (Fig. 9(b)). In this way, when MAM is constituted by a PZT, Fig. 9(a) shows with a blue line the continuous voltage, equivalent to $v_o[s(t)] = 0.0192$ Vrms, which was harvested at the output of the MAM when we generated a sinusoidal signal, $s(t)$, at 500 Hz by using an acoustic source. Also, with a red line, Fig. 9(a), shows the continuous voltage, equivalent to $v_o[n(t)] = 0.0124$ Vrms, which was harvested at the output of the MAM when we generated a pink noise signal by using an acoustic source, $n(t)$. Thus, when $v_o[s(t)] = 0.0192$ Vrms we measured $v_i[s(t)] = 0.126$ Vrms at the output of the acoustic source. But, when $v_o[n(t)] = 0.0124$ Vrms, we measured $v_i[n(t)] = 0.0794$ Vrms at the output of the acoustic source. Note that the output of the acoustic source is equivalent to the input of the MAM. It is worth noting that, when $s(t)$ is considered, and the MAM is constituted by a PZT, the effective gain offered by MAM is $\gamma_{s(t)} = 0.1523$, but when $n(t)$ is considered $\gamma_{n(t)} = 0.1561$.

On the other hand, when an HR constitutes MAM with a PZT embedded in it, Fig. 9(b) shows with blue line the continuous voltage, equivalent to $v_o[s(t)] = 0.212$ Vrms, harvested at the output of the MAM when a sinusoidal signal, $s(t)$, at 500 Hz was generated by the acoustic source. Also, with a red line Fig. 9(b) shows the continuous voltage, equivalent to $v_o[n(t)] = 0.159$ Vrms, harvested at the output of the MAM, when a pink noise signal, $n(t)$, is generated by the acoustic source. Thus, when $v_o[s(t)] = 0.212$ Vrms then $v_i[s(t)] = 0.126$ Vrms was measured at the output of the acoustic source. But, when $v_o[n(t)] = 0.159$ Vrms then $v_i[n(t)] = 0.0794$ Vrms was measured at the output of the acoustic source. Note that the output of the acoustic source is equivalent to the input of the MAM. Considering that $\gamma = v_o/v_i$, where v_o is the RMS output voltage and v_i is the RMS voltage when the input signal is $s(t)$ or $n(t)$, and the MAM is constituted by an HR with a PZT embedded in it, the effective gain offered by MAM is $\gamma_{s(t)} = 1.683$, but when $n(t)$ is

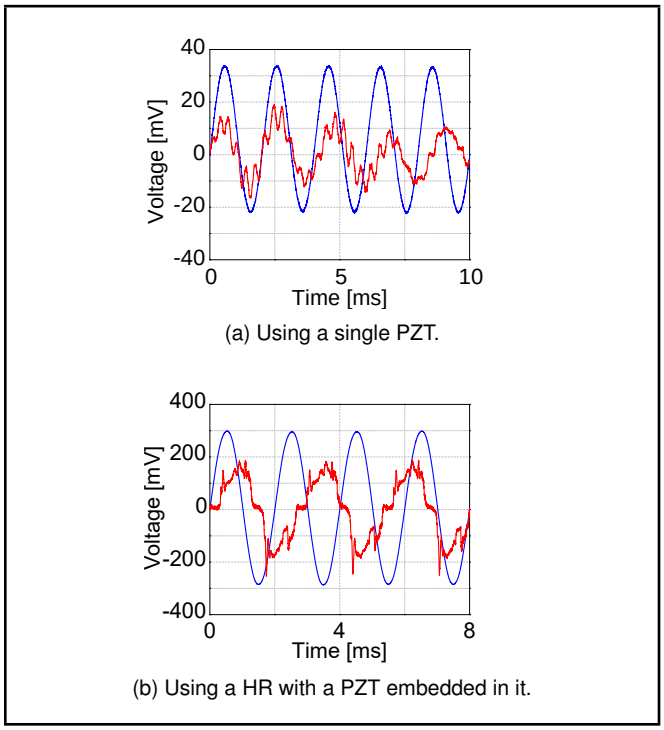

Figure 9. Harvested voltage using the implemented EHS when v_i is a pure sinusoidal signal at 500 Hz, $s(t)$ (blue line), or v_i is a pink noise signal, $n(t)$ (red line): a) the MAM is a PZT and b) the MAM consists of a PZT embedded inside a HR.

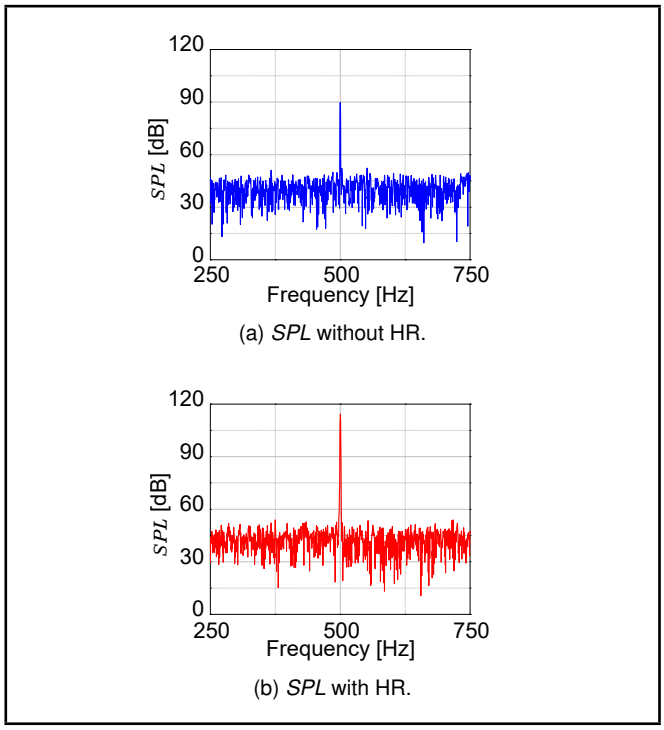

Figure 10. Sound pressure level (SPL) at implemented HR using a pure sinusoidal signal wrapped in environmental noise.

considered $\gamma_{n(t)} = 2.003$.

We should note that when an HR constitutes MAM with a PZT embedded in it, its effective gain is greater than the effective gain of the MAM constituted by a PZT. With the two analyzed cases, the measured amplification gain of the HR is $K_m = 11.051$ when the acoustic source generated $s(t)$, but $K_m = 12.872$ when the acoustic source generated $n(t)$.

Another alternative for experimentally measuring the amplification gain of the HR can be established from Fig. 10, which shows the sound pressure level (SPL) measured at the output of the acoustic source by using a sound level meter. Thus, Fig. 10(a) shows the SPL measured at the output of acoustic source generating a sinusoidal signal at 500 Hz wrapped in environmental noise, and Fig. 10(b) shows the SPL inside of the HR chamber when the acoustic source generates a sinusoidal signal at 500 Hz wrapped in environmental noise. Now, considering that $SPL\,(500\text{ Hz}) = 90$ dB in Fig. 10(a) and $SPL\,(500\text{ Hz}) = 112.64$ dB in Fig. 10(b), the amplification gain of HR is $K_m = 13.55$.

Note that the amplification factors of HR experimentally measured $K_m(s(t))$ and $K_m(n(t))$ are nominally very similar in magnitude. But when we use an acoustic source that generates a sinusoidal signal at 500 Hz wrapped in environmental noise, $K_m = 13.55$ is the most reliable amplification gain of HR because the measurements are based on SPL and not based on root mean square voltages.

7.2. Energy Harvesting under Real Conditions

For actual conditions, the acoustic source in Fig. 7 is replaced by environmental noise. The results show an increase in the harvested voltage compared to those obtained under controlled conditions. These results closely agree with the voltage signals generated in controlled conditions, which confirms the analysis discussed in the previous section since these depict well-defined voltage levels.

In Fig. 11, we showed the voltage levels harvested from the PZT under actual conditions at music and vehicular traffic locations. In Fig. 11(a), we showed approximately the harvested voltage level of 282.8 mVrms in a music location. In Fig. 11(b), we showed the harvested voltage level in a traffic location where the voltage level obtained was approximately 318.15 mVrms.

The voltage levels are higher when considering real conditions using the implemented HR. Under real conditions, we can observe a greater variation in the harvested energy since, in the two environments studied, there are impulsive noises that provide voltage peaks to have a greater harvested energy. From the average sound pressure levels shown in Table 2, we estimated the equivalent voltage generated by the acoustic source in $v_i(m(t)) = 47.31$ mVrms, when $m(t)$ is the sound generated in a music location; and $v_i(g(t)) = 199.5$ mVrms, when $g(t)$ is the sound generated in a vehicular traffic location. Considering these estimated values and the harvested voltage $v_o(m(t)) = 281.8$ mVrms and $v_o(g(t)) = 318.15$ mVrms for each case, the effective gains of the proposed system were $\gamma_{m(t)} = 5.977$ for the music location and $\gamma_{g(t)} = 1.595$ for the vehicular traffic location.

8. DISCUSSION

From the challenges of developing new devices for energy harvesting, which should maintain the balance between the health of the environment and the use of natural resources, the need arises for guidelines to assist engineering students and practitioners in developing innovative eco-friendly devices that generate clean energy. Therefore, it is necessary to allow interested students and practitioners to create innovative prod-

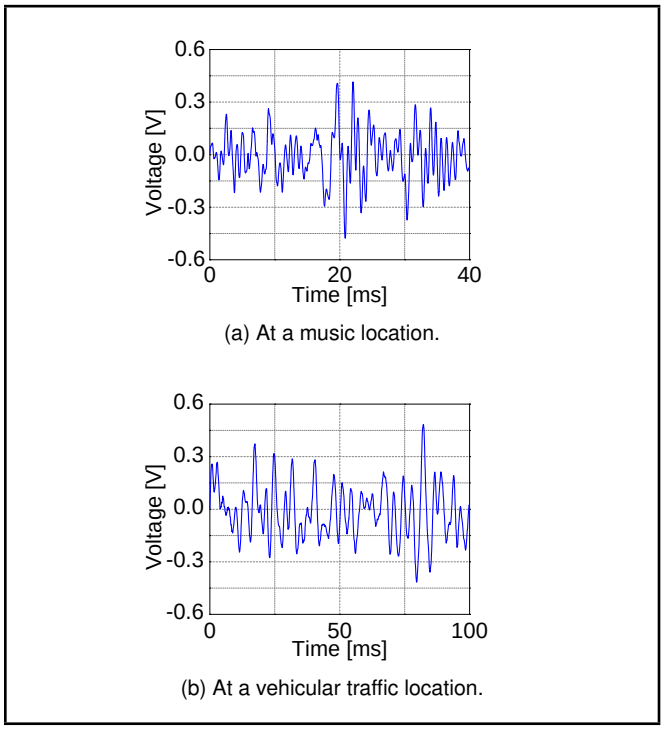

Figure 11. Harvested voltage under real conditions using the implemented EHS.

ucts based on non-conventional energy sources. In this way, we seek to show that obtaining clean and valuable energy is possible. Regarding energy harvesters, although development and innovation can be defined by the circumstances and physical and geographical conditions in which the energy harvesting is done, this work can help employ piezo-acoustic devices seeking the highest efficiency in energy harvesting, considering sustainable alternatives. This work is helpful because it establishes the basis for designing systems that harvest energy at small scales, from environmental noise or other viable sources for applications with low-consumption energy.

We emphasize some differences between the systems mentioned in Section 3 against the EHS implemented in this work. These differences are due to the sound intensity level, the type of acoustic source, HR dimensions, and the materials used to implement each system, as well as the conditions established for each of the performed experiments. Considering all these aspects, we show in the following that the proposed EHS is competent in voltage harvesting compared to other systems. In contrast, the system has a unique module to harvest energy from environmental noise. With the idea of establishing a comparison of the implemented EHS against other approaches that harvest energy from environmental noise, we have considered three works: Li *et al.*,[3] Li *et al.*,[4] and Pillai and Ezhilarasi.[6]

Firstly, we must emphasize that our EHS is a simple and compact system that consists of a single PZT embedded in a mechanical amplifier. In contrast, the systems considered in the comparison consist of arrays of PZTs. In Table 4, we can observe that the system proposed by Li *et al.*[4] includes eight PZTs using an acoustic source producing a sound pressure level (SPL) at 110 dB, the system proposed by Li *et al.*[3] includes ten PZTs using an acoustic source at 100 dB, and the system proposed by Pillai and Ezhilarasi[6] includes a triangular foil with a modified PZT using an acoustic source at 98 dB. Thus, Table 4 shows that the EHSs proposed by Li *et al.*[3,4] and by Pillai and Ezhilarasi[6] harvest a higher voltage than the implemented EHS. However, we must consider that the sound pressure levels used by them are higher than those used for the system proposed in this work.

Table 4. Harvested voltage reported for the considered EHSs when compared against the implemented EHS.

SPL Source	V_{out} [volts]	Number of PZTs	Reference
110 dB	15.680	Ten	Li *et al.*[3]
98 dB	0.920	One	Pillai and Ezhilarasi[6]
100 dB	1.480	Eight	Li *et al.*[4]
90 dB	0.212	One	System proposed

Table 5. Estimated energy harvested when the acoustic source produces a sound pressure level at 90 dB.

System	Estimated harvested voltage		
	Eight PZTs [volts]	Ten PZTs [volts]	One PZT [volts]
Other systems	1.609[3]	0.147[4]	0.920[6]
Proposed system	1.696	2.120	0.212

Now, to fairly compare our EHS against those EHSs under consideration, we have estimated the harvested voltage for the systems developed by Li *et al.*[3,4] and by Pillai and Ezhilarasi[6] considering that the acoustic source produces an SPL at 90 dB. The harvested voltages estimated for these cases are reported in Table 5, and they were calculated considering Eq. 14:

$$SPL = 20\log(\frac{V_{\text{out}}}{V_{\text{ref}}}). \tag{14}$$

Thus, for V_{out} and SLP values reported on Table 4, we calculated the actual values for V_{ref} in all cases, and using these values for V_{ref}, we calculated the hypothetical values for V_{out} considering that the assumed acoustic sources produce an SPL at 90 dB.

We note that our EHS would be able to harvest a higher voltage than that harvested by the other systems when the acoustic source produces 90 dB. Note that when the three devices are evaluated under similar conditions, the energy harvesting obtained with the approach developed in this work is comparable to and surpasses the devices designed by Li *et al.*[3,4] Thus, it is worth noting that if the developed EHS is scaled, it will show good performance considering the voltages harvested by the devices shown in Table 5.

In the same sense, now we have estimated the harvested voltage by our EHS when the acoustic source produces 98, 100, and 110 dB as for other systems used for comparison purposes. The harvested voltages estimated for these cases are reported in Table 6. It should be noted that our EHS would be able to harvest a higher voltage than the voltage harvested by the EHSs developed by Li *et al.*[3,4] On the other hand, when the proposed EHS is evaluated considering an acoustic source producing a sound pressure level at 98 dB, the harvested voltage is lower than that obtained using the system developed by Pillai and Ezhilarasi.[6] We emphasize that the method produced by Pillai and Ezhilarasi[6] has a better performance than our EHS as it is composed of a high-performance PZT.

9. CONCLUSIONS

The approach with which this work is presented constitutes a methodology that establishes the necessary concepts to guide

Table 6. Estimated energy harvesting considering different sound pressure level conditions for the acoustic source.

System	Estimated harvested voltage		
	@98 dB [volts]	@100 dB [volts]	@110 dB [volts]
Proposed system	0.532	6.700	16.952
Li *et al.*	–	1.480[4]	15.680[3]
Pillai and Ezhilarasi	0.920[6]	–	–

engineering students and practitioners in analyzing, designing, and implementing systems for energy harvesting from environmental noise based on piezoelectric films and mechanical resonators. With the concepts presented in this work, we have shown the way to obtain the electrical parameters of the piezoelectric film, the equations useful for the Helmholtz resonator sizing, and the analysis and measurement of environmental noise at different locations. We also showed the necessary components to perform each of the experiments defined for measuring the harvested energy levels under controlled and actual conditions. This work constitutes a theoretical-practical guideline that produces a functional system for energy harvesting from environmental noise. This work shows a practical method to design and implement a system that harvests energy from environmental noise, which is based on a mechanical amplifier designed to operate around a frequency of 500 Hz and is based on a piezoelectric transducer (PZT) embedded inside a Helmholtz resonator (HR). The proposed system is based on characterizing the PZT S118-J1SS-1808YB and determining its resonant frequency. Then, with this information, the physical dimensions of the HR were calculated. The implementation of this HR offers an experimentally measured amplification gain between 11.05 and 13.55.

Three options were used to estimate the amplification gain of the HR: i) when the acoustic source generates a pure sinusoidal signal at 500 Hz, considering the relation between the RMS equivalent voltage measured inside HR and the RMS equivalent voltage measured at the output of the acoustic source, ii) when the acoustic source generates a pink noise signal, also considering the relation between the RMS equivalent voltage measured inside HR and the RMS equivalent voltage measured at the output of the acoustic source, and iii) when the acoustic source generates a pure sinusoidal signal at 500 Hz wrapped in environmental noise considering the relation between the SPL was measured at the input and inside of the mechanical amplifier. The last option of measuring the amplification gain was considered more reliable than the other two options because the estimation is based on the SPL at the input and within the HR. The proposed EHS was operated in two test scenarios. In the first test scenario, the system harvested energy under controlled experimental conditions considering a pure sinusoidal signal at 500 Hz and a pink noise signal. Both signals were generated from an acoustic source consisting of a function generator, an electrical signal amplifier, and a loudspeaker. In this case, the proposed EHS offered an effective gain between 168.3% and 200.3%. In the second test scenario, the implemented EHS harvested energy under actual conditions considering two locations: a music location and a vehicular traffic location. For the music location, the proposed system offered an effective gain of 597.7% and for the vehicular traffic location of 159.5%. Considering the harvested energy, the proposed EHS was compared against the EHSs presented by other authors, and two cases were established.

In the first case, we estimated the harvested voltage if we would use the EHSs proposed by Li *et al.*[3,4] considering the same SPL conditions used in the proposed EHS; that is, we assumed that the acoustic source produces 90 dB. In this case, the proposed EHS proved to perform better than the EHSs used in the comparison. In the second case, we estimated the harvested voltage if we would use the proposed EHS considering the same SPL conditions used in the EHSs proposed by Li *et al.*[3,4] and the EHS presented by Pillai and Ezhilarasi;[6] that is, we assumed that the acoustic source produces 98, 100, and 110 dB. In this estimation, we can note that the proposed EHS harvested a higher voltage than other EHSs, assuming that the acoustic source produces an SPL of 100 dB and 110 dB. However, the proposed EHS harvested a lower amount of voltage than another system, assuming that the acoustic source produces an SPL of 98 dB. Based on the results obtained in this work, it is confirmed that the harvested energy through an EHS, such as the EHS proposed here, can be harnessed in low-power applications. In addition, this work offers the possibility of establishing the feasibility of a scaling-up of the proposed EHS. This fact can be seen from the estimated harvested energy, assuming that the proposed EHS can be incorporated into an array with the idea of harvesting a more significant amount of energy. This work also shows an alternative to harnessing the existing noise pollution in large cities to produce valuable energy.

CONTRIBUTIONS

D. Aguilar-Torres and O. Jiménez-Ramírez, performed the computations, designed, and built the energy harvesting system. D. Aguilar-Torres, J. A. Jimenez-Garcia, G. Luque-Zuñiga, and O. Flores-Acoltzi designed the study case. O. Jiménez-Ramírez and R. Vázquez-Medina devised the project and the main conceptual ideas, and they developed the required theory. All authors discussed the results and contributed to the final manuscript.

FUNDING

Instituto Politécnico Nacional, (IPN-Mexico) [Grant numbers SIP-20220531 (R. Vázquez-Medina) and SIP-20220572 (O. Jiménez-Ramírez)].

ACKNOWLEDGEMENTS

D. Aguilar-Torrez (CVU-829790) and G. Luque-Zúñiga (CVU-717933) thank for scholarship provided by Consejo Nacional de Ciencia y Tecnología (Mexico).

STATEMENTS AND DECLARATIONS

The authors declare no conflict of interest. The founders had no role in the design of the study; in the collection, analyses, or interpretation of data; in the writing of the manuscript, or in the decision to publish the results.

REFERENCES

[1] Ilas, A., Ralon, P., Rodríguez, A., and Taylor, M. *Renewable power generation costs in 2017*, International Renewable Energy Agency, Abu Dhabi, United

Arab Emirates, ISBN 978-92-9260-040-2, Retrieved from https://www.irena.org/publications, (2018).

[2] Kiziroglou, M. E. and Yeatman, E. M. Materials and techniques for energy harvesting, *Functional Materials for Sustainable Energy Applications*, Elsevier, London, UK, Chapter 17, 541–572, (2012). https://doi.org/10.1533/9780857096371.4.539

[3] Li, B., Laviage, A. J., You, J. H., and Kim, Y.-J. Harvesting low-frequency acoustic energy using quarter-wavelength straight-tube acoustic resonator, *Applied Acoustics*, **74** (11), 1271–1278, (2013). https://doi.org/10.1016/j.apacoust.2013.04.015

[4] Li, B., You, J. H., and Kim, Y.-J. Low frequency acoustic energy harvesting using PZT piezoelectric plates in a straight tube resonator, *Smart Materials and Structures*, **22** (5), 055013(9), (2013). https://doi.org/10.1088/0964-1726/22/5/055013

[5] Li, Z., Chen, H., Zou, H., and Li, J. Research progress of cavity-based acoustic energy harvester, *Journal of Vibroengineering*, **23**, 1680–1693, (2021). https://doi.org/10.21595/jve.2021.22057

[6] Pillai, M. A. and Ezhilarasi, D. Improved acoustic energy harvester using tapered neck Helmholtz resonator and piezoelectric cantilever undergoing concurrent bending and twisting, *Procedia Engineering*, **144**, 674–681, (2016). https://doi.org/10.1016/j.proeng.2016.05.065

[7] Izhar and Khan, F. U. Three degree of freedom acoustic energy harvester using improved Helmholtz resonator, *International Journal of Precision Engineering and Manufacturing*, **19**, 143–154, (2018). https://doi.org/10.1007/s12541-018-0017-z

[8] Wang, Y., Zhu, X., Zhang, T., Bano, S., Pan, H., Qi, L., Zhang, Z., and Yuan, Y. A renewable low-frequency acoustic energy harvesting noise barrier for high-speed railways using a Helmholtz resonator and a PVDF film, *Applied Energy*, **230**, 52–61, (2018). https://doi.org/10.1016/j.apenergy.2018.08.080

[9] Gao, M. Y., Wang, P., Cao, Y., Chen, R., and Liu, C. A railborne piezoelectric transducer for energy harvesting of railway vibration, *Journal of Vibroengineering*, **18** (7), 4647–4663, (2016). https://doi.org/10.21595/jve.2016.16938

[10] Shan, X., Tian, H., Chen, D., and Xie, T. A curved panel energy harvester for aeroelastic vibration, *Applied Energy*, **249**, 58–66, (2019). https://doi.org/10.1016/j.apenergy.2019.04.153

[11] Bo, L. D. and Gardonio, P. Energy harvesting with electromagnetic and piezoelectric seismic transducers: Unified theory and experimental validation, *Journal of Sound and Vibration*, **433**, 385–424, (2018). https://doi.org/10.1016/j.jsv.2018.06.034

[12] Bolat, F. C., Basaran, S., and Sivrioglu, S. Piezoelectric and electromagnetic hybrid energy harvesting with low-frequency vibrations of an aerodynamic profile under the air effect, *Mechanical Systems and Signal Processing*, **133**, 106246, (2019). https://doi.org/10.1016/j.ymssp.2019.106246

[13] Jiang, L., Yang, Y., Chen, R., Lu, G., Li, R., Li, D., Humayun, M. S., Shung, K. K., Zhu, J., Chen, Y., and Zhou, Q. Flexible piezoelectric ultrasonic energy harvester array for bio-implantable wireless generator, *Nano Energy*, **56**, 216–224, (2019). https://doi.org/10.1016/j.nanoen.2018.11.052

[14] Nabavi, S. F., Farshidianfar, A., Afsharfard, A., and Khodaparast, H. H. An ocean wave-based piezoelectric energy harvesting system using breaking wave force, *International Journal of Mechanical Sciences*, **151**, 498–507, (2019). https://doi.org/10.1016/j.ijmecsci.2018.12.008

[15] Priya, S. Advances in energy harvesting using low profile piezoelectric transducers, *Journal of Electroceramics*, **19** (1), 167–184, (2007). https://doi.org/10.1007/s10832-007-9043-4

[16] Zou, H., Chen, H., and Zhu, X. Piezoelectric energy harvesting from vibrations induced by jet-resonator system, *Mechatronics*, **26**, 29–35, (2015). https://doi.org/10.1016/j.mechatronics.2015.01.002

[17] Ballato, A. Piezoelectricity: history and new thrusts, *Proc. of the IEEE Intternational Ultrasonics Symposium*, USA, 575–583, (1996). https://doi.org/10.1109/ULTSYM.1996.584046

[18] Cupich-Rodríguez, M. and Elizondo-Garza, F. J. Actuadores piezoeléctricos, *Ingenierías* (in Spanish), **3** (6), 22–28, (2000).

[19] Castellanos, N. Evaluación preliminar del uso del efecto piezoeléctrico para generación de energía, *INVENTUM* (in Spanish), **8** (15), 35–40, (2013). https://doi.org/10.26620/uniminuto.inventum.8.15.2013.35-40

[20] Elhalwagy, A. M., Ghoneem, M. Y. M., and Elhadidi, M. Feasibility study for using piezoelectric energy harvesting floor in buildings interior spaces, *Energy Procedia*, **115**, 114–126, (2017). https://doi.org/10.1016/j.egypro.2017.05.012

[21] Ilyas, M. A. and Swingler, J. Towards a prototype module for piezoelectric energy harvesting from raindrop impacts, *Energy*, **125**, 716–725, (2017). https://doi.org/10.1016/j.energy.2017.02.071

[22] Maamer, B., Boughamoura, A., El-Bab, A. M. R. F., Francis, L. A., and Tounsi, F. A review on design improvements and techniques for mechanical energy harvesting using piezoelectric and electromagnetic schemes, *Energy Conversion and Management*, **199**, 111973, (2019). https://doi.org/10.1016/j.enconman.2019.111973

[23] Sarker, M. R., Julai, S., Sabri, M. F. M., Said, S. M., Islam, M. M., and Tahir, M. Review of piezoelectric energy harvesting system and application of optimization techniques to enhance the performance of the harvesting system, *Sensors and Actuators A: Physical*, **300**, 111634, (2019). https://doi.org/10.1016/j.sna.2019.111634

[24] Choi, J., Jung, I., and Kang, C.-Y. A brief review of sound energy harvesting, *Nano Energy*, **56**, 169–183, (2019). https://doi.org/10.1016/j.nanoen.2018.11.036

[25] Fang, L. H., Hassan, S. I. S., Rahim, R. A., Isa, M., and bin Ismail, B. Exploring piezoelectric for sound wave as energy harvester, *Energy Procedia*, **105**, 459–466, (2017). https://doi.org/10.1016/j.egypro.2017.03.341

[26] Fang, L. H., Hassan, S. I. S., Rahim, R. A., Isa, M., and Bin Ismail, B. Charaterization of differents dimension piezoelectric transducer for sound wave energy harvesting, *Energy Procedia*, **105**, 836–843, 2017. https://doi.org/10.1016/j.egypro.2017.03.398

[27] Mir, F., Saadatzi, M., Ahmed, R. U., and Banerjee, S. Acoustoelastic MetaWall noise barriers for industrial application with simultaneous energy harvesting capability, *Applied Acoustics*, **139**, 282–292, (2018). https://doi.org/10.1016/j.apacoust.2018.04.029

[28] Noh, H.-M. Acoustic energy harvesting using piezoelectric generator for railway environmental noise, *Advances in Mechanical Engineering*, **10** (7), 168781401878505, (2018). https://doi.org/10.1177/1687814018785058

[29] Ahmad, I., Hassan, A., Anjum, M. U., Malik, S., and Ali, T. Ambient acoustic energy harvesting using two connected resonators with piezoelement for wireless distributed sensor network, *Acoustical Physics*, **65** (5), 471–477, (2019). https://doi.org/10.1134/S1063771019050014

[30] Hu, G., Tang, L., and Cui, X. On the modelling of membrane-coupled Helmholtz resonator and its application in acoustic metamaterial system, *Mechanical Systems and Signal Processing*, **132**, 595–608, (2019). https://doi.org/10.1016/j.ymssp.2019.07.017

[31] Eghbali, P., Younesian, D., and Farhangdoust, S. Enhancement of the low-frequency acoustic energy harvesting with auxetic resonators, *Applied Energy*, **270**, 115217, (2020). https://doi.org/10.1016/j.apenergy.2020.115217

[32] Ponche, R., Hascoet ,J. Y., Kerbrat, O., and Mognol, P. A new global approach to design for additive manufacturing, *Virtual and Physical Prototyping*, **7** (2), 93–105, (2012). https://doi.org/10.1080/17452759.2012.679499

[33] Orquéra, M., Campocasso, S., and Millet, D. Design for additive manufacturing method for a mechanical system downsizing, *Procedia CIRP* **60**, 223–228, (2017). https://doi.org/10.1016/j.procir.2017.02.011

[34] Liu, G., Xiong, Y., and Rosen, D. W. Multidisciplinary design optimization in design for additive manufacturing, *Journal of Computational Design and Engineering*, **9** (1), 128–143, (2022). https://doi.org/10.1093/jcde/qwab073

[35] Bruneau, M. *Fundamentals of Acoustics*, John Wiley & Sons, Newport Beach, CA, USA, ISBN 10:1-905209-25-8, (2013).

[36] Torres, D. A., Medina, R. V., Jasso, E. G., and Ramírez, O. J. Piezoelectric transducers and their application to harvesting of energy produced by environmental noise, *Proc. of the International Energy Conference 2019*, 270–277, Academia Mexicana de Energía A. C., ISSN: 2448-5624, (2019).

[37] Kinsler, L. E., Frey, A. R., Coppens, A. B., and Sanders, J. V. *Fundamentals of Acoustics*, John Wiley & Sons, Hoboken, NJ, USA, ISBN: 978-0-471-84789-2, (2000).

[38] de Kluijver, H. and Stoter, J. Noise mapping and GIS: optimising quality and efficiency of noise effect studies, *Computers, Environment and Urban Systems*, **27** (1), 85–102, (2003). https://doi.org/10.1016/S0198-9715(01)00038-2

[39] Secretaria de Medio Ambiente y Recursos Naturales (MX), Norma Oficial Mexicana-NOM-081-SEMARNAT-1994: Límites máximos permisibles de emisión de ruido de las fuentes fijas y su método de medición, Retrieved from https://www.dof.mx, (2013).

[40] Safari, A. and Akdogan, E. K. (Eds.) *Piezoelectric and Acoustic Materials for Transducer Applications*, Springer Science & Business Media, New York, USA, ISBN: 978-0-387-76538-9, (2003).

[41] Gomez-Meda, R., Measurement of the Thiele-Small parameters for a given loudspeaker, without using a box, *AES Convention*, Audio Engineering Society, **91**, 1–16, Retrieved from http://www.aes.org/e-lib/browse.cfm?elib=5554, (1991).

[42] Struck, C. J. Determination of the Thiele-Small parameters using two-channel FFT Analysis, *AES Convention*, Audio Engineering Society, **82**, 1–25, Retrieved from http://www.aes.org/e-lib/browse.cfm?elib=4983, (1987).

[43] Gokcek, C. Tracking the resonance frequency of a series RLC circuit using a phase locked loop, *Proc. of 2003 IEEE Conference on Control Applications*, 609–613, (2003). https://doi.org/10.1109/CCA.2003.1223506

[44] Fuchs, H. V. *Applied Acoustics: Concepts, Absorbers, and Silencers for Acoustical Comfort and Noise Control*, Springer Science & Business Media, Berlin, Germany, (2013). https://doi.org/10.1007/978-3-642-29367-2

[45] Komkin, A. I., Mironov, M. A., and Bykov, A. I. Sound absorption by a Helmholtz resonator, *Acoustical Physics*, **63**, 356–363, (2017). https://doi.org/10.1134/S1063771017030071

[46] Blackstock, D. T. *Fundamentals of Physical Acoustics*, Acoustical Society of America, USA, ISBN: 0471319791, (2001).

[47] Nédélec, J. C. The Helmholtz Equation, In: *Acoustic and Electromagnetic Equations*, Springer, New York, NY, ISBN: 978-1-4419-2889-4, (2001). https://doi.org/10.1007/978-1-4757-4393-7

[48] Mechel, F. P. (Ed.), Munjal, M. L., Vorlander, M., Koltzsch, P., Ochmann, M., Cummings, A., Maysenholder, W., and Arnold, W. *Formulas of Acoustics*, Springer Science & Business Media, ISBN: 978-3-540-76832-6, (2008).